Journal of Chromatography, 590 (1992) 147–151
Elsevier Science Publishers B.V., Amsterdam

CHROMSYMP. 2418

Glucose–fructose equilibria on Dowex Monosphere 99 CA resin under overloaded conditions

M. Saska*, S. J. Clarke, Mei Di Wu and K. Iqbal

Audubon Sugar Institute/Sugar Station, Louisiana State University Agricultural Center, Baton Rouge, LA 70803 (USA)

ABSTRACT

Matching of the numerical simulation of the band propagation with experimental elution profiles of glucose and fructose was used to obtain the adsorption isotherms of glucose and fructose at 70°C on Dowex Monosphere 99 CA resin (Dow Chemical), an adsorbent widely used in the high-fructose corn syrup (HFCS) industry. The respective distribution coefficients, $K_G = 0.245 + 0.0051c_G + 0.003c_F$ and $K_F = 0.47 + 0.007c_G + 0.0049c_F$, are non-linear and dependent on the concentrations of both sugars. Contrary to some previous reports, the height equivalent to a theoretical plate of glucose (2.7 cm) was less than that of fructose (3.5 cm). The ideal chromatographic model with the band spreading originating in an implicit way from the numerical integration of the appropriate partial differential equation was found suitable to fit the coupled, non-linear behavior of glucose–fructose mixtures and can be a useful tool for modelling and optimization of the industrial simulated moving bed HFCS process.

INTRODUCTION

The continuous simulated moving bed (SMB) fructose-selective adsorption separation of glucose–fructose mixtures has been a standard process in high-fructose corn syrup (HFCS) production for a decade. In the last 2 years, using the potassium form of sulphonated polystyrene resins, the technology has been applied on an industrial scale to the de-sugarization of sugarbeet molasses (ion-exclusion) and, pending resolution of problems with pretreatment of the more impure sugarcane solutions, it also promises new possibilities in the sugarcane industry.

For reliable modeling and design of a large-scale SMB operation, it is crucial to understand the properties of the adsorbent, *viz.*, adsorption equilibria (partition coefficients) and mass transfer rates. These should be determined preferably by pulse testing [1] on the SMB system itself or a scalable pilot plant to account correctly not only for the properties of the adsorbent but also for the band broadening from column connections and valves and column packing characteristics. Care should be taken that the loading, flow-rates and range of concentrations in the tests are comparable to the conditions prevailing in the SMB process. It was shown recently [2] that the frequently made assumption of linear and uncoupled isotherms of glucose and fructose on Ca^{2+} polystyrene resins may not be valid at high concentrations (see Table I) and that it affects considerably the predicted steady-state profile within an SMB system. This in turn leads to operational parameters (switching time and flow-rates) that, if based on the model, result in less than optimum separation.

In this paper we report results of measuring the adsorptive properties of a Dowex Monosphere 99 CA resin (Ca^{2+} form; Dow Chemical, Midland, MI, USA) for glucose and fructose under conditions of high concentrations. The isotherms obtained were used to model the SMB separation of glucose–fructose mixtures.

EXPERIMENTAL

The SMB pilot plant at Audubon Sugar Institute consists of eight identical jacketed glass columns (210 cm × 6 cm I.D., column volume 5940 ml) connected with a series of either computer- or manually operated solenoid valves and sampling ports. The pulse tests were done on either six or seven in-series connected columns, packed with

0021-9673/92/$05.00

Dowex Monosphere 99 CA resin (particle size 0.32 mm, 6% cross-linked) and kept at 70°C, by first feeding the top of the first column with predetermined amounts (±1 g) of fructose–glucose solutions of various compositions and then eluting the components with hot deionized water (*ca.* 75°C) at flow-rates between 120 and 160 ml/min (±0.1 ml/min). The direction of the flow was downwards in all columns to eliminate problems with fluidizing the resin bed [7]. The elution time was measured from the moment of switching the water pump on. The samples were then taken periodically and their concentration (refractive index) determined off-line. High-performance liquid chromatographic (HPLC) analysis (Aminex HPX-87N column, Bio-Rad Labs.) was used with two-component feeds. In the high-load tests (*e.g.*, runs 5, 6, 11 and 12 in Fig. 2), columns one (runs 5 and 12) and one and two in series (runs 6 and 12) were used as feed reservoirs by feeding these columns with the feed until the outlet reached the inlet composition. Then a connection was made with the remainder of the columns and the feed eluted as before.

The response signals were integrated numerically to give the mean and variance of the elution peaks:

$$t' = \int ct\,dt / \int c\,dt \tag{1}$$

$$\sigma^2 = \int c(t - t')^2\,dt / \int c\,dt \tag{2}$$

The chromatographic height equivalent to a theoretical plate (HETP) was calculated as $L'(\sigma/t')^2$, where the total column length L was corrected for the length of the feed "plug" L_f as

$$L' = L - \tfrac{1}{2}L_f = L - \tfrac{1}{2}m_f/(\rho\varepsilon A)$$

where ρ is the feed density and A the column cross-sectional area. In high-load tests, L_f was taken as L or $2L$ (L = column length, 210 cm) depending on whether one or two columns were equilibrated initially with the feed. Thus, in the HFCS experiments, the load with respect to fructose was higher (by the excess in the solid phase) than would correspond to the HFCS composition.

The assumed form of the distribution coefficients was as before (Table I):

$$K_G \equiv q_G/c_G = K_{G0} + A_1c_G + B_1c_F \tag{3}$$

$$K_F \equiv q_F/c_F = K_{F0} + A_2c_G + B_2c_F \tag{4}$$

where c is the liquid concentration (g per 100 ml) and q the concentration in the resin (g per 100 ml of resin), and the coefficients were obtained by matching the experimental profiles with those calculated from a local equilibrium model:

$$\partial c/\partial t + [(1 - \varepsilon)/\varepsilon]\partial q/\partial t + v(\partial c/\partial z) = 0 \tag{5}$$

The time and space partial derivatives were replaced as usual with finite differences of the forward and backward types, respectively, and solved on a Model 386-based PC. The non-linearities stemming from the form of the distribution coefficients were accommodated with an internal iteration procedure. The time and length integration steps, 0.8 min and 10 cm, of the discretized eqn. 5 were chosen such as to match the profiles of low-concentration pulse responses (Fig. 1) and thus substitute for the lack of explicit axial dispersion terms (axial mixing and mass transfer) in the master equation. The slight underestimation of the peak heights of glucose (see also Fig. 3) indicates that the band broadening (and HETP) is less than that of fructose and therefore slightly different integration steps should be used for the two sugars.

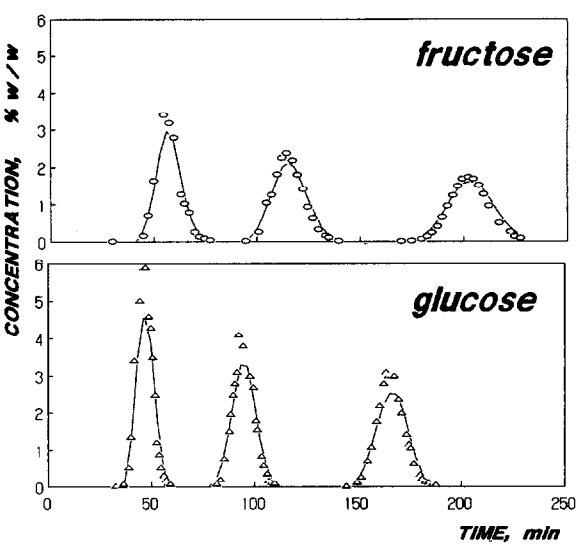

Fig. 1. Experimental (symbols) and calculated (solid lines) elution profiles of (○) fructose and (△) glucose (single-component feeds). A total of six in-series columns were used, with sampling after two, four and six columns. Fructose experiment: c_f = 19.8%, q = 146.5 ml/min. Glucose experiment: c_f = 23.6%, q = 150.2 ml/min. K_{G0} = 0.245; A_1 = 0.0051; K_F^0 = 0.47; B_2 = 0.0049.

K_{G0} and K_{F0} were obtained by matching the low-concentration feed profiles (single-component feeds) with those calculated while neglecting the concentrationn dependent terms of the distribution coefficients ($A_1 = A_2 = B_1 = B_2 = 0$). A_1 and B_2 were obtained from single-component runs with feed concentrations from 15 to 60 wt.% (with $A_2 = B_1 = 0$), and the cross-coefficients, A_2 and B_1 were obtained from runs where the feed was an HFCS syrup diluted to between 10 and 60% (w/w). The system void fraction, $\varepsilon = 0.47$, which includes the column connections, valves, etc., was found from pulse tests with a high-molecular-weight dextran.

RESULTS AND DISCUSSION

The HETP evaluated from runs 1–4 and 7–10 is 2.7 ($\sigma = 0.5$, $N = 4$) and 3.5 cm ($\sigma = 0.2$, $N = 4$) for glucose and fructose, respectively, about one third of those found by Ching and Ruthven [4] on smaller columns.

The retention time (empty column bed volumes eluted at the peak maxima) generally increases (Fig. 2) with increasing column load (proportional to the feed volume and concentration), although the volume-averaged concentrations of the bands as they move through the column should prove a more meaningful parameter in correlating the retention times.

The average values of the parameters determined here fall within the ranges found previously for similar resins (Table I):

$$K_G = 0.245 + 0.0051c_G + 0.003c_F \quad (6)$$

$$K_F = 0.47 + 0.007c_G + 0.0049c_F \quad (7)$$

The separation on the Dowex Monosphere 99 CA resins, judged by the K_{F0}/K_{G0} ratio of 1.92 at 70°C, appears to be superior to that on Duolite resins at the same temperature (Table I).

The upward curvature of the isotherms causes the characteristic "sharpening" of the fructose band (Fig. 3): while the tail ($c_G = 0$) is made steeper because $B_2 > 0$ (a low-concentration element of the solutions trqvels faster that a high-concentration element, *i.e.*, the peak of the band), the broadening of the front (that would be expected in a single component band) is countered by the effect of glucose, *i.e.*, the front of the fructose band is slowed

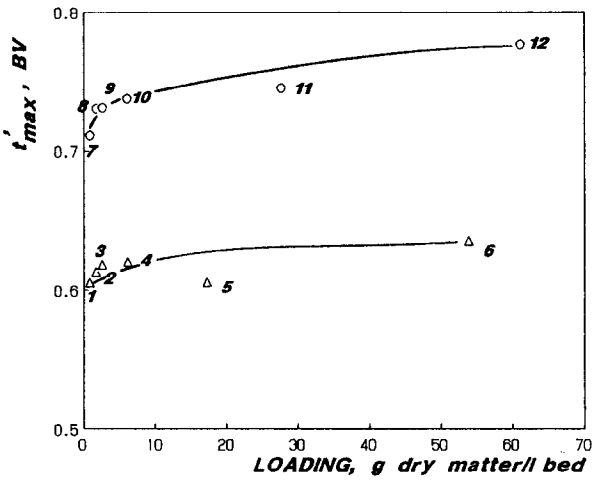

Fig. 2. Retention times ($qt'_{max}/L'A$) in bed volumes at the peak maxima at different column loadings. Single-component feeds. The run parameters for experiments 1–12 were as follows [experiment No. (c_f, % dry matter; dry matter fed, g; L_f, cm)]: 1 (11.0; 33; 11); 2 (20.5; 62.5; 11); 3 (30.4; 96.7; 11); 4 (60.5; 219; 11); 5 (16.8; 668; 210); 6 (20; 1603; 420); 7 (10; 30; 11); 8 (20.4; 62.6; 11); 9 (29.7; 95.0; 11); 10 (59.7; 217.9; 11); 11 (20.0; 905; 210); 12 (20.0; 1814; 240).

on account of glucose relative to the velocity of the maximum of the fructose band.

The non-linearity and dependence of the isotherms can be qualitatively understood by considering the limited accessibility of the internal surface of the resin to the sugar molecules. The volume-weighted median pore size (diameter) of the resin is *ca.* 10 Å (manufacturer's information), *i.e.*, half of the total volume of the pores is composed of pores smaller than 10 Å and half of pores larger than 10 Å. Therefore, a large fraction of the pores have diameters rougly equal to the diameter of the hydrated sugar molecules. Penetration into these micropores then involves displacing the hydration layers of the counter ions and also, perhaps, those of the diffusing sugar molecules, a process favoured by the increasing sugar concentration in the liquid and by the diminishing concentration of the water molecules at high sugar concentrations. The degree of hydration and the diameter of the hydrated sugar clusters are known to be less at high sugar concentrations. The contraction of the resin at high sugar concentrations (Fig. 4) may also be expected, however, to contribute at least partially to the non-linearities. Whereas the pore volume and mean pore size are likely to

TABLE I

PARTITION COEFFICIENT OF GLUCOSE (K_G) AND FRUCTOSE (K_F) ON SEVERAL SULPHONATED POLYSTYRENE RESINS IN THE Ca^{2+} FORM

$K_G = K_{G0} + A_1c_G + B_1c_F$; $K_F = K_{F0} + A_2c_G + B_2c_F$. A zero indicates that this parameter was not determined (a linear model was assumed *a priori*) rather than that is was determined to be zero.

Sorbent	Ref.	T (°C)	K_{G0}	A_1	B_1	K_{F0}	A_2	B_2	K_{F0}/K_{G0}
Dowex 50W-X8	3	30	0.30	0	0	0.80	0	0	2.7
Zerolit 225 SRC 14	4	20	0.20	0	0	0.78	0	0	3.9
		30	0.20	0	0	0.67	0	0	3.4
		48	0.20	0	0	0.56	0	0	2.8
		60	0.20	0	0	0.49	0	0	2.5
Duolite C204	5	29	0.5	0	0	0.88	0	0	1.8
		52.5	0.5	0	0	0.75	0	0	1.5
		70	0.5	0	0	0.67	0	0	1.3
Korela VO7C	6		0.215	0	0	0.472	0	0	2.2
Duolite C204	7	25	0.51	0	0	0.88	0	0	1.7
Zerolit SRC14	8, 9	25	0.126	0.0039	0.0042	0.38	0.0065	0.00075	3.0
Duolite C204	2	55	0.36	0.001	0.0015	0.465	0.0015	0.0025	1.3
Duolite C204F	10	60	0.374	0	0	0.468	0	0	1.3
Dowex Monosphere 99 CA	This work	70	0.245	0.0051	0.003	0.47	0.007	0.0049	1.9

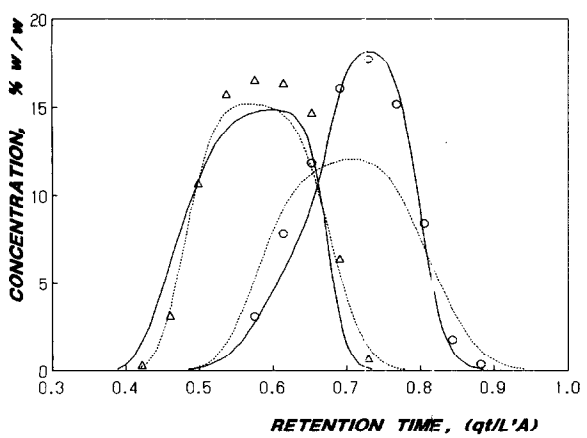

Fig. 3. Measured elution profiles [(△) glucose; (○) fructose] and thise calculated from the non-linear model (solid lines): K_{G0} = 0.245; A_1 = 0.0051; B_1 = 0.001; K_{F0} = 0.47; A_2 = 0.01; B_2 = 0.0049. Dotted lines represent a "best" linear model: K_{G0} = 0.35; K_{F0} = 0.60; $A_1 = A_2 = B_1 = B_2 = 0$. q = 135 ml/min; feed, 30% (w/w) HFCS.

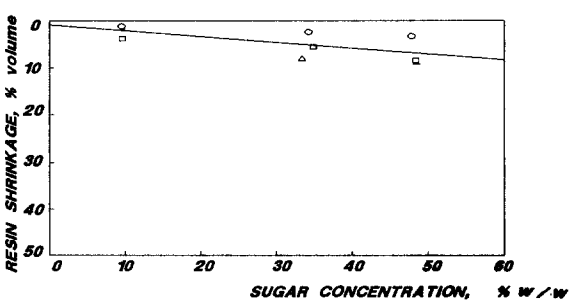

Fig. 4. Shrinkage of the resin beads at 25°C and various sugar concentrations (△ = glucose; ○ = fructose; □ = sucrose; two experimental points for glucose, at concentrations 9.5 and 48.5%, are obscured by other points). Dowex Monosphere 99 CA resin. Determination by direct measurement of the beads diameters at high magnifications [11]. The solid line is the least-squares fit of all points.

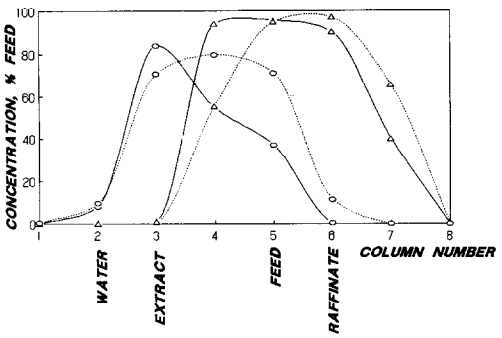

Fig. 5. Simulated steady-state SMB profiles (△ = glucose; ○ = fructose) for linear (dotted lines) and non-linear (solid lines) isotherms. Parameters as listed in Fig. 3. Feed, 30% HFCS; flow-rates, feed 23.3 ml/min (0.029 BV/h (BV = bed volume)), water 46.6 (0.059), extract (fructose product) 28.3 (0.036), raffinate (glucose product) 41.7 (0.053), recycle 100 (0.126); switching time, linear 30.4 min, non-linear 28.8 min; total bed volume, 47.52 l. System configuration: water, in column 2; extract, out of column 3; feed, in column 5; raffinate, out of column 6.

decrease as a result of bead contraction and thus contribute to a Langmuir-type behaviour, the bed void fraction may not be a constant as assumed in the above partial differential equation but rather an increasing function of concentration. This would then be expected to contribute to the upward curvature of the isotherms.

As expected, the simulated steady-state SMB profiles differ significantly depending on the assumed adsorption characteristics of the components (Fig. 5). If known accurately under the conditions prevailing in the SMB process, they can in turn be used to optimize the SMB separation. The simulation can be handled with a fast personal computer [12] and thus provide an accessible tool for efficient operation.

REFERENCES

1 A. deRosset, R. W. Neuzil and D. J. Korous, *Ind. Eng. Chem., Process Des. Dev.*, 15 (1976) 261.
2 C. B. Ching, C. Ho, K. Hidajat and D. M. Ruthven, *Chem. Eng. Sci.*, 42 (1987) 2547.
3 Y. S. Ghim and H. N. Chang, *Ind. Eng. Chem., Fundam.*, 21 (1982) 369.
4 C. B. Ching and D. M. Ruthven, *Can. J. Chem. Eng.*, 62 (1984) 398.
5 C. B. Ching and D. M. Ruthven, *Chem. Eng. Sci.*, 41 (1986) 3063.
6 P. E. Barker and G. Ganetsos, *J. Chem. Tech. Biotechnol.*, 35 (1985) 217.
7 C. B. Ching and D. M. Ruthven, *Chem. Eng. Sci.*, 40 (1985) 877.
8 P. E. Barker and S. Thawait, *J. Chromatogr.*, 295 (1984) 479.
9 D. M. Ruthven, *J. Chromatogr.*, 351 (1986) 337.
10 V. Viard and M. L. Lameloise, *Récents Progrès en Génie des Procédés*, Vol. 8a, Lavoisier, Paris, 1989, p. 233.
11 M. Mrini, *M.S. Thesis*, Louisiana State University, Baton Rouge, LA, in progress.
12 M. Saska, unpublished results.